Communication

Potassium 6-oxo-7,13,16,22-tetraazatetracyclo[12.6.2.18,12.017,21]tricosa-1(20),8(23),9,11,14,16,18,21-octaen-2-yne-15-carboxylate

Camille Blouet , Stéphanie Letast , Thomas Robert , Stéphane Bach , Noël Pinaud , Nicolas Joubert , Marie-Claude Viaud-Massuard , Jean Guillon , Cédric Logé , Caroline Denevault-Sabourin *

Posted Date: 11 September 2023

doi: 10.20944/preprints202309.0598.v1

Keywords: macrocycle; quinoxaline; Pim kinases; kinase inhibitor

Communication

Potassium 6-Oxo-7,13,16,22-tetraazatetracyclo[12.6.2.1^{8,12}.0^{17,21}]tricosa-1(20),8(23),9,11,14,16,18,21-octaen-2-yne-15-carboxylate

Camille Blouet [1], Stéphanie Letast [1], Thomas Robert [2,3], Stéphane Bach [2,3,4], Noël Pinaud [5], Nicolas Joubert [1], Marie-Claude Viaud-Massuard [1], Jean Guillon [6], Cédric Logé [7] and Caroline Denevault-Sabourin [1,*]

1 Research Center for Respiratory Diseases (CEPR), Team: "Proteolytic Mechanisms in Inflammation", University of Tours, INSERM, UMR 1100, F-37032 Tours, France; camille.blouet@etu.univ-tours.fr (C.B.); nicolas.joubert@univ-tours.fr (N.J.); marie-claude.viaud-massuard@univ-tours.fr (M.-C.V.-M.); caroline.denevault@univ-tours.fr (C.D.-S.)
2 Integrative Biology of Marine Models Laboratory (LBI2M), Sorbonne University, CNRS, UMR8227, F-29680 Roscoff, France; trobert@sb-roscoff.fr (T.R.); bach@sb-roscoff.fr (S.B.)
3 Kinase Inhibitor Specialized Screening facility (KISSf), Sorbonne University, CNRS, FR2424, F-29680 Roscoff, France
4 Centre of Excellence for Pharmaceutical Sciences, North-West University, Private Bag X6001, Potchefstroom 2520, South Africa
5 ISM, University of Bordeaux, CNRS, UMR 5255, F-33405 Talence, France; noel.pinaud@u-bordeaux.fr (N.P.)
6 ARNA Laboratory, University of Bordeaux, INSERM U12132-UMR CNRS 5320, F-33076 Bordeaux, France; jean.guillon@u-bordeaux.fr (J.G.)
7 Department of Medicinal Chemistry, IICIMED-UR1155, IRS2, Nantes University, F-44200 Nantes, France; cedric.loge@univ-nantes.fr (C.L.)
* Correspondence: caroline.denevault@univ-tours.fr; Tel.: +33-2-47-36-72-31

Abstract: Potassium 6-oxo-7,13,16,22-tetraazatetracyclo[12.6.2.1^{8,12}.0^{17,21}]tricosa-1(20),8(23),9,11,14,16,18,21-octaen-2-yne-15-carboxylate was synthesized through a multi-step pathway starting from commercially available 3-iodo-1,2-phenylenediamine. Structure characterization of this new substituted macrocyclic quinoxaline compound was achieved by using ^{1}H NMR, ^{13}C NMR, and HRMS spectral analysis. This new macrocyclic derivative demonstrated submicromolar potency on both Pim-1 and Pim-2 isoforms, with an interesting selectivity profile against a selected panel of human kinases.

Keywords: macrocycle; quinoxaline; Pim kinases; kinase inhibitor

1. Introduction

Pim (Provirus Integration site for Moloney murine leukemia virus) kinases are a family of three constitutively active proto-oncogenic serine/threonine protein kinases (Pim-1, Pim-2 and Pim-3), regulating various cellular processes, including cell proliferation, survival and differentiation [1,2]. Because, they share a certain level of sequence homology, they can activate similar cellular pathways and can sometimes be considered as compensatory proteins [2,3]. However, these kinases present individual characteristics, especially in their tissue distribution [4]. Pim kinases are implicated in oncogenesis, particularly in tumor progression and metastasis, and are considered as important drivers of chemotherapy resistance [5]. Thus, these kinases are overexpressed in a large variety of tumors, with differences in their expression pattern according to the cancer type. Thereby, while Pim-1 and Pim-2 are commonly up-regulated in hematopoietic cancers [6–10], Pim-3 is mostly over-expressed in some solid cancers (e.g. prostate cancers) [11]. Finally, mice deficient for all Pim kinases

Preprints (www.preprints.org) | NOT PEER-REVIEWED | Posted: 11 September 2023 doi:10.20944/preprints202309.0598.v1

displayed mild phenotypic modifications, including reduced body size and impaired responses to hematopoietic growth factors [12,13], demonstrating the interest of targeting these kinases in oncology. Moreover, crystal structures of Pim-1 and Pim-2 revealed unique particularities in comparison to others kinases, which can be exploited to develop selective Pim inhibitors [14,15].

In this context, and in the course of our drug discovery program on the development of new targeted antileukemic treatments, we previously identified the new quinoxaline lead compound **1**, acting as a submicromolar dual Pim1/2 inhibitor (IC_{50} of 130 nM and 170 nM, on Pim-1 and Pim-2, respectively) (Figure 1), but displaying also micromolar inhibition of DYRK1A and GSK3β off-target mammalian kinases [16]. In the light of these results, we decided to prepare optimized analogues of compound **1**, with an improved selectivity profile. Thus, taking into account our experience on the structure-activity relationships (SAR) in our previously described quinoxaline derivatives series [16,17], we used the quinoxaline-2-carboxylic acid scaffold as a template for the design and the synthesis of a new macrocyclic compound. SAR and molecular modeling studies highlighted the crucial role of the carboxylic acid moiety in position 2 for the Pim kinase inhibitory activity, establishing a key salt bridge with the catalytic lysine residue of Pim1/2 kinases at physiological pH. Moreover, macrocycles have been emerging as a valuable class of pharmacological agents over the past decade. Indeed, macrocyclization allows restriction of the conformational freedom observed in small molecules, permitting to optimize affinity and selectivity [18], and macrocyclic kinase inhibitors have reached advanced clinical trial, particularly in oncology [19,20]. In 2021, the Food and Drug Administration approved lorlatinib, the first macrocyclic kinase inhibitor in metastatic anaplastic lymphoma kinase (ALK)-positive non-small cell lung cancer. Here, we report the synthesis and structural identification of the potassium 6-oxo-7,13,16,22-tetraazatetracyclo[12.6.2.1^{8,12}.0^{17,21}]tricosa-1(20),8(23),9,11,14,16,18,21-octaen-2-yne-15-carboxylate **8**. This original macrocyclic quinoxaline **8** was further evaluated on human Pim-1 and Pim-2 kinases and on a selected panel of human protein kinases, to determine its selectivity profile.

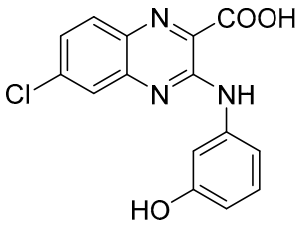

Lead compound 1

Pim-1 IC_{50} = 130 nM
Pim-2 IC_{50} = 170 nM

Figure 1. Chemical structure of lead compound **1**.

2. Results and Discussion

2.1. Potassium 6-oxo-7,13,16,22-tetraazatetracyclo[12.6.2.1^{8,12}.0^{17,21}]tricosa-1(20),8(23),9,11,14,16,18,21-octaen-2-yne-15-carboxylate

The synthesis of the potassium 6-oxo-7,13,16,22-tetraazatetracyclo[12.6.2.1^{8,12}.0^{17,21}]tricosa-1(20),8(23),9,11,14,16,18,21-octaen-2-yne-15-carboxylate **8** was performed as described in Scheme 1.

First, intermediate **3** was synthesized in two steps. The peptide coupling reaction between commercially available pent-4-ynoic acid and *tert*-butyl (3-aminophenyl)carbamate in *N*,*N*-dimethylformamide (DMF), using 1-[Bis(dimethylamino)methylene]-1*H*-1,2,3-triazolo[4,5-*b*]pyridinium 3-oxid hexafluorophosphate (HATU) and 2,6-lutidine, gave the carbamate intermediate **2**, which was then deprotected, in a 10% trifluoroacetic acid (TFA) solution to provide the attempted trifluoroacetic salt **3**.

Preprints (www.preprints.org) | NOT PEER-REVIEWED | Posted: 11 September 2023 doi:10.20944/preprints202309.0598.v1

The preparation of 3-chloro-5-iodoquinoxaline key intermediate **5a** was then achieved in two steps according to literature procedures [16,17,21,22]. Briefly, commercial 3-iodo-1,2-phenylenediamine was condensed with diethyl 2-oxomalonate, in ethanol, using citric acid as catalyst to give ester **4a**, which was separated from its 8-iodo isomer **4b** by silica column chromatography. Chlorination in position 3 of esters **4a** and **4b** was realized, using DMF as a catalyst, in refluxing phosphorous oxychloride to give the corresponding esters **5a** and **5b**. Intermediate **5b**, in contrast with its isomer **5a**, gave a yellow single crystal, which was used for the 3D structural determination by X-ray crystallography (Figure 2), to identify the position of the iodo group on the quinoxaline scaffold in the solid state of this isomer, confirming the structure of each isomer.

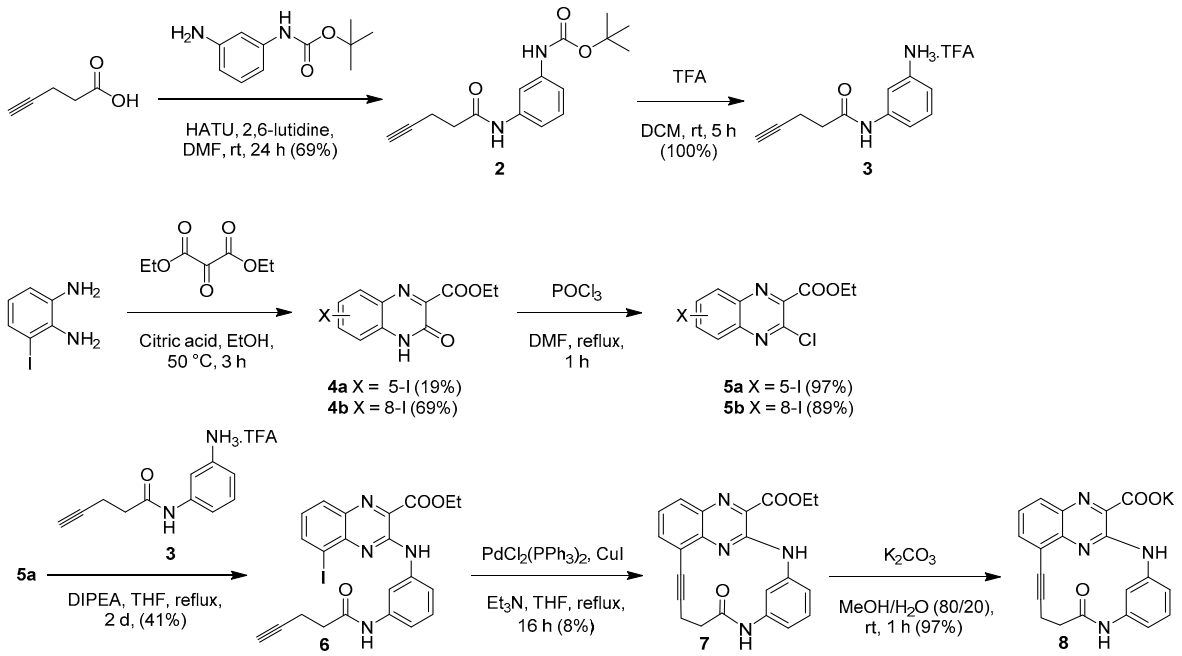

Scheme 1. Synthesis of Potassium 6-oxo-7,13,16,22-tetraazatetracyclo[12.6.2.1^{8,12}.0^{17,21}]tricosa-1(20),8(23),9,11,14,16,18,21-octaen-2-yne-15-carboxylate (**8**).

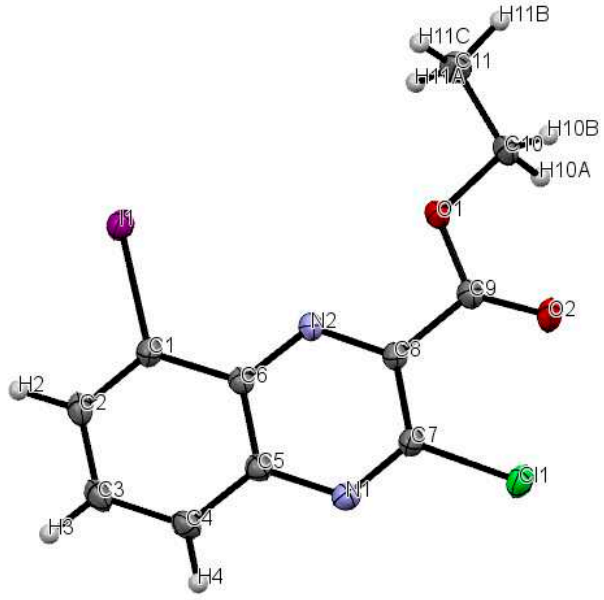

Figure 2. The ORTEP (Oak Ridge Thermal Ellipsoid Plot) drawing of ethyl 3-chloro-8-iodoquinoxaline-2-carboxylate (**5b**) with thermal ellipsoids at 30% level.

Preprints (www.preprints.org) | NOT PEER-REVIEWED | Posted: 11 September 2023 doi:10.20944/preprints202309.0598.v1

Access to the macrocyclic quinoxaline **8** was then performed, using a three-step synthetic pathway. After treatment of trifluoroacetic salt **3** with *N*,*N*'-diisopropylethylamine (DIPEA), the resulting amine derivative was then engaged in a nucleophilic aromatic substitution reaction with quinoxaline **5a**, in refluxing dry tetrahydrofuran (THF), to yield intermediate **6**, which underwent an intramolecular Sonogashira cross-coupling reaction, using $PdCl_2(PPh_3)_2$, and CuI, as catalysts, and triethylamine in refluxing THF, leading to the macrocyclic quinoxaline **7**. Hydrolysis of ethyl ester **7** with potassium carbonate in 80% aqueous methanol was then performed to afford the macrocyclic potassium salt **8**. The structure of this new macrocyclic quinoxaline derivative **8** was then confirmed by ^{1}H NMR, and HRMS analysis (see Supplementary Materials).

2.2. Protein Kinase Assays

The ability of the macrocyclic quinoxaline **8** to inhibit the *in vitro* enzymatic activity of human Pim-1 and Pim-2, and of a selected panel of six human off-target protein kinases (comprising DYRK1A, CDK5/p25, CDK9/CyclinT, Haspin, CK1ε and GSK3β), was evaluated, using a luminescence-based kinase assay [23]. The commercially available pan-Pim protein kinase inhibitor, SGI-1776 [24], was used as a control for the *in vitro* studies. As shown in Table 1, compound **8** displayed a submicromolar activity on Pim-1 and Pim-2 (IC_{50} of 400 nM, and 100 nM, respectively) with the same level of activity on Pim-2 but a slightly decreased activity on Pim-1, in comparison to lead compound **1** and SGI-1776, the reference drug. However, the general selectivity profile of macrocycle **8** on the panel of human protein kinases studied was significantly improved in comparison to compound **1** and SGI-1776. Indeed, while compound **1** displayed low micromolar inhibition of DYRK1A and GSK3β, and SGI-1776 potently inhibited five of the six human kinases tested (IC_{50} values of 0.05 to 9.53 μM), compound **8** displayed an interesting selectivity profile against the six potential off-target kinases (CDK5/p25, CDK9/CyclinT, Haspin, CK1ε and GSK3β), with IC_{50} inhibition values > 10 μM in every case.

Table 1. Kinase selectivity profile of compounds **1** and **8**.

Compound	Kinase enzymatic IC_{50} (μM) [a]							
	Pim-1	**Pim-2**	**DYRK1A**	**CDK5/p25**	**CDK9/ CyclinT**	**Haspin**	**CK1ε**	**GSK3β**
1	0.13	0.17	2.58	> 10	> 10	> 10	> 10	2.80
8	0.40	0.10	> 10	> 10	> 10	> 10	> 10	> 10
SGI-1776	0.05	0.10	3.80	9.53	1.08	0.05	6.54	> 10

[a] IC_{50} on disease-related kinase activity were calculated from dose-response curves. Each inhibitor concentration was tested in duplicate. All protein kinases used here are human. DYRK1A: dual specificity tyrosine phosphorylation regulated kinase 1A, CDK: cyclin-dependent kinase, Haspin: haploid germ cell-specific nuclear protein kinase, CK1: casein kinase 1, GSK3: glycogen synthase kinase 3.

3. Materials and Methods

All solvents were anhydrous reagents from commercial sources. Unless otherwise noted, all chemicals and reagents were obtained commercially and used without purification. Melting points (m.p.) were determined on a Stuart capillary apparatus and are uncorrected. High-resolution mass spectra (HRMS) were performed on a Bruker maXis mass spectrometer by the SALSA platform from ICOA laboratory, in positive mode with an ESI source. NMR spectra were recorded at 400 MHz (^{1}H), 101 MHz (^{13}C) or 376 MHz (^{19}F) on a Bruker Avance (400 MHz) spectrometer. The chemical shifts are reported in parts per million (ppm, δ) relative to residual deuterated solvent peaks. The abbreviations s = singlet, d = doublet, t = triplet, q = quadruplet, m = multiplet and bs = broad signal were used throughout.

3.1. Tert-butyl (3-(pent-4-ynamido)phenyl)carbamate (2)

To a solution of pent-4-ynoic acid (106 mg, 1.08 mmol) in dry N,N-dimethylformamide (DMF) (3 mL), under an argon atmosphere, were added 1-[Bis(dimethylamino)methylene]-1H-1,2,3-triazolo[4,5-b]pyridinium 3-oxid hexafluoro-phosphate (HATU) (680 mg, 1.79 mmol) in solution in dry DMF (3 mL) and 2,6-lutidine (207 µL, 1.79 mmol), and the resulting mixture was stirred magnetically at room temperature for 10 minutes. Tert-butyl (3-aminophenyl)carbamate (188 mg, 0.90 mmol) was then added and the mixture was stirred at room temperature for 24 h. The solvent was then removed under reduced pressure, and the residue was finally purified by silica column chromatography using cyclohexane with ethyl acetate gradient (0-60%) as eluent, to give compound **2** (214 mg, 69%) as a white powder, m.p. 130 °C. ^{1}H NMR (400 MHz, DMSO-d6) δ 9.91 (s, 1H), 9.32 (s, 1H), 7.78 (s, 1H), 7.29 (d, J = 8.4 Hz, 1H), 7.13 (dd, J = 8.4, 8.8 Hz, 1H), 7.02 (d, J = 8.8 Hz, 1H), 2.78 (t, J = 2.4 Hz, 1H), 2.50-2.40 (m, 4H), 1.47 (s, 9H). ^{13}C NMR (101 MHz, DMSO-d6) δ 169.2, 152.7, 139.8, 139.4, 128.7, 113.3, 113.0, 109.1, 83.7, 78.9, 71.4, 35.1, 28.1 (3 × C), 14.1.

*3.2. 3-(Pent-4-ynamido)benzenaminium trifluoroacetic salt (**3**)*

To a solution of compound **2** (1.20 g, 4.16 mmol,) in dichloromethane (DCM) (40 mL) was added dropwise a 10% trifluoroacetic acid (TFA) solution (4 mL) at 0 °C. The resulting mixture was stirred magnetically at 0 °C for 30 minutes, and then, at room temperature for 5 h. The solvent was then removed under reduced pressure, and the residue was finally purified by silica column chromatography using DCM with methanol (MeOH) gradient (0-15%) as eluent, to give compound **3** (1.19 g, 100%) as a brown oil. ^{1}H NMR (400 MHz, DMSO-d6) δ 10.01 (s, 1H), 7.50 (s, 1H), 7.20 (dd, J = 8.4, 7.6 Hz, 1H), 7.12 (d, J = 8.4 Hz, 1H), 6.69 (d, J = 7.6 Hz, 1H), 4.25-3.00 (m, 3H), 2.79 (t, J = 2.4 Hz, 1H), 2.55-2.40 (m, 4H). ^{13}C NMR (101 MHz, DMSO-d6) δ 169.8, 140.2, 134.7, 130.0, 116.7, 116.3, 112.2, 83.6, 71.5, 35.2, 14.1. ^{19}F NMR (376 MHz, DMSO-d6) δ -74.1 (s).

3.3. Ethyl 5-iodo-3-oxo-3,4-dihydroquinoxaline-2-carboxylate (4a) and ethyl 8-iodo-3-oxo-3,4-dihydroquinoxaline-2-carboxylate (4b)

A mixture of 3-iodo-1,2-phenylenediamine (1.00 g, 4.27 mmol), diethyl 2-oxomalonate (0.81 mL, 5.31 mmol) and citric acid (132 mg, 0.69 mmol) in ethanol (50 mL) was stirred magnetically at 50 °C for 3 h. Ethanol was then evaporated under reduced pressure, and the resulting residue was purified by silica column chromatography using cyclohexane with ethyl acetate gradient (0-70%) as eluent to give compound **4a** (275 mg, 19%) and its 8-iodo isomer **4b** (1.01 g, 69%) as yellow powders.

*Compound **4a***: m.p. 162 °C. ^{1}H NMR (400 MHz, DMSO-*d6*) δ 11.54 (bs, 1H), 8.21 (d, *J* = 6.0 Hz, 1H), 7.90 (d, *J* = 7.6 Hz, 1H), 7.24 (dd, *J* = 7.6, 6.0 Hz, 1H), 4.39 (q, *J* = 7.2 Hz, 2H), 1.33 (t, *J* = 7.2 Hz, 3H).

*Compound **4b***: m.p. 238 °C. ^{1}H NMR (400 MHz, DMSO-*d6*) δ 12.96 (bs, 1H), 7.89 (dd, *J* = 4.4, 2.4 Hz, 1H), 7.37-7.29 (m, 2H), 4.39 (qd, *J* = 7.2, 2.0 Hz, 2H), 1.33 (td, *J* = 7.2, 2.0 Hz, 3H).

3.4. Ethyl 3-chloro-5-iodoquinoxaline-2-carboxylate (5a)

Method A: into a dry three-neck round bottom flask was introduced compound **4a** (100 mg, 0.29 mmol) in phosphorous oxychloride (0.96 mL) at ice bath temperature. The mixture was vigorously stirred magnetically at 0 °C for 5 min and DMF (42 µL) was then added at 0 °C and the reaction mixture was refluxed for 1 h. After cooling at 0 °C, the resulting mixture was neutralized with a 1 M sodium hydroxide aqueous solution, and extracted with ethyl acetate. The combined organic layers were washed with brine, and dried over $MgSO_4$, filtered, and evaporated under reduced pressure to obtain derivative **5a** (102 mg, 97%) as a yellow solid, m.p. 120 °C. ^{1}H NMR (400 MHz, DMSO-*d6*) δ 8.61 (dd, *J* = 7.6, 1.2 Hz, 1H), 8.23 (dd, *J* = 8.4, 1.2 Hz, 1H), 7.75 (dd, *J* = 8.4, 7.6 Hz, 1H), 4.50 (q, *J* = 7.2 Hz, 2H), 1.39 (t, *J* = 7.2 Hz, 3H). ^{13}C NMR (101 MHz, DMSO-*d6*) δ 162.9, 144.8, 143.9, 143.0, 141.7, 139.7, 133.0, 129.9, 100.7, 62.8, 13.9.

 doi:10.20944/preprints202309.0598.v1

3.5. Ethyl 3-chloro-8-iodoquinoxaline-2-carboxylate (5b)

The title compound was synthesized according to the general method A from compound **4b** (100 mg, 0.29 mmol), phosphorous oxychloride (0.96 mL) and DMF (42 µL). Compound **5b** was obtained (94 mg, 89%) as a yellow solid, m.p. 105 °C. ^{1}H NMR (400 MHz, DMSO-*d6*) δ 8.55 (dd, *J* = 7.2, 0.8 Hz, 1H), 8.10 (dd, *J* = 8.4, 0.8 Hz, 1H), 7.75 (dd, *J* = 8.4, 7.2 Hz, 1H), 4.52 (qd, *J* = 7.2, 1.6 Hz, 2H), 1.40 (td, *J* = 7.2, 1.6 Hz, 3H). ^{13}C NMR (101 MHz, DMSO-*d6*) δ 163.4, 145.4, 144.1, 142.4, 142.2, 139.7, 134.8, 129.3, 102.9, 63.3, 14.4.

3.6. Ethyl 5-iodo-3-((3-(pent-4-ynamido)phenyl)amino)quinoxaline-2-carboxylate (6)

To a solution of trifluoroacetic salt **3** (160 mg, 0.56 mmol) and *N,N'*-diisopropylethylamine (DIPEA) (500 µL, 2.87 mmol) in dry tetrahydrofuran (THF) (3 mL), under an argon atmosphere, was added dropwise compound **5a** (64 mg, 0.18 mmol) in solution in dry THF (1 mL). The resulting mixture was refluxed for 2 days. The solvent was then removed under reduced pressure, and the residue was finally purified by silica column chromatography using cyclohexane with ethyl acetate gradient (0-100%) as eluent to give intermediate **6** (37 mg, 41%) as a yellow powder, m.p. 127 °C. ^{1}H NMR (400 MHz, DMSO-*d6*) δ 10.36 (s, 1H), 9.99 (s, 1H), 8.56 (d, *J* = 8.4 Hz, 1H), 8.38 (dd, *J* = 7.6, 1.2 Hz, 1H), 8.02 (dd, *J* = 8.0, 1.2 Hz, 1H), 7.92 (s, 1H), 7.41-7.32 (m, 2H), 7.22 (d, *J* = 8.8 Hz, 1H), 4.51 (q, *J* = 7.2 Hz, 2H), 2.82 (t, *J* = 2.4 Hz, 1H), 2.59-2.50 (m, 4H), 1.43 (t, *J* = 7.2 Hz, 3H). ^{13}C NMR (101 MHz, DMSO-*d6*) δ 169.5, 165.2, 148.6, 142.3, 142.1, 139.5, 139.1, 135.5, 133.3, 130.2, 129.3, 127.6, 115.0, 114.3, 110.8, 98.5, 83.7, 71.5, 62.5, 35.2, 14.1, 14.0.

3.7. Ethyl 6-oxo-7,13,16,22-tetraazatetracyclo[12.6.2.1^{8,12}.0^{17,21}]tricosa-1(20),8(23),9,11,14,16,18,21-octaen-2-yne-15-carboxylate (7)

Into a sealed tube were introduced bis(triphenylphosphine)palladium(II) dichloride ($PdCl_2(PPh_3)_2$) (4 mg , 5.7 µmol), copper iodide (CuI) (0.3 mg, 1.6 µmol) and triethylamine (16 µL, 0.12 mmol) in dry THF (3 mL), under an argon atmosphere. Then, intermediate **6** (20 mg, 39 µmol) was added dropwise, and the reaction mixture was refluxed for 16 h. The solvent was then removed under reduced pressure, and the residue was finally purified by silica column chromatography using cyclohexane with ethyl acetate gradient (0-100%) as eluent to give the macrocycle **7** (1.2 mg, 8%), as a yellow oil. ^{1}H NMR (400 MHz, DMSO-*d6*) δ 10.16 (s, 1H), 9.60 (s, 1H), 9.48 (bs, 1H), 7.97 (dd, *J* = 8.4, 0.8 Hz, 1H), 7.87 (dd, *J* = 7.2, 0.8 Hz, 1H), 7.53 (dd, *J* = 8.4, 7.2 Hz, 1H), 7.34 (t, *J* = 8.0 Hz, 1H), 7.06 (dd, *J* = 8.0, 1.6 Hz, 1H), 6.79 (dd, *J* = 8.0, 1.6 Hz, 1H), 4.50 (q, *J* = 7.2 Hz, 2H), 2.95 (t, *J* = 5.6 Hz, 2H), 2.59 (t, *J* = 5.6 Hz, 2H), 1.42 (t, *J* = 7.2 Hz, 3H). ^{13}C NMR (101 MHz, DMSO-*d6*) δ 172.7, 165.2, 147.9, 142.6, 139.6, 139.3, 135.4, 135.0, 132.5, 129.3, 129.0, 126.1, 120.4, 119.0, 118.6, 116.8, 95.5, 78.6, 62.4, 29.0, 16.2, 14.0. HRMS (ESI) *m/z*: [M+H]+ calcd for $C_{22}H_{19}N_4O_3$, 387.14572; found 387.14516.

3.8. Potassium 6-oxo-7,13,16,22-tetraazatetracyclo[12.6.2.1^{8,12}.0^{17,21}]tricosa-1(20),8(23),9,11,14,16,18,21-octaen-2-yne-15-carboxylate (8)

To ester **7** (1 mg, 2.6 µmol) in aqueous methanol (80%, 2 mL), potassium carbonate (0.36 mg, 2.6 µmol) was added and the reaction mixture was stirred magnetically at room temperature for 1 h. After cooling, MeOH was removed under reduced pressure, and the aqueous phase was washed with ethyl acetate, and evaporated under reduced pressure to yield macrocycle **8** (1 mg, 97%) as a yellow powder, m.p. > 350 °C. ^{1}H NMR (400 MHz, DMSO-*d6*) δ 13.29 (s, 1H), 9.62 (s, 1H), 9.61 (bs, 1H), 7.86 (dd, *J* = 8.0, 1.2 Hz, 1H), 7.66 (d, *J* = 7.2, 1.2 Hz, 1H), 7.38 (dd, *J* = 8.0, 7.2 Hz, 1H), 7.28 (t, *J* = 8.0 Hz, 1H), 6.86 (d, *J* = 8.0, 2.0 Hz, 1H), 6.70 (dd, *J* = 8.0, 2.0 Hz, 1H), 2.94 (t, *J* = 4.8 Hz, 2H), 2.65 (t, *J* = 4.8 Hz, 2H). HRMS (ESI) *m/z*: [M+2H]+ calcd for $C_{20}H_{15}N_4O_3$, 359.11442, found 359.11401.

3.9. X-Ray Data

The structure of compound **5b** was established by X-ray crystallography (Figure 2). The yellow single crystal of **5b** was obtained by slow evaporation from a methanol/chloroform solution (*v/v* : 20/80): triclinic, space group P-1, a = 6.6838(5) Å, b = 8.6592(6) Å, c = 10.5128 (7) Å, α = 79.521(2)°, β =

89.243(2)°, γ = 86.626(2)°, V = 597.26 (7)Å^3, Z = 2, δ(calcd) = 2.016 Mg.m^{-3}, FW = 362.54 for $C_{11}H_8ClIN_2O_2$, F(000) = 348. Full crystallographic results have been deposited at the Cambridge Crystallographic Data Centre (CCDC-2262892), UK, as supplementary material [25]. The data were corrected for Lorentz and polarization effects and for empirical absorption correction [26]. The structure was solved by direct methods Shelx 2013 [27] and refined using Shelx 2013 [27] suite of programs.

3.10. Protein Kinase Assays

Kinase enzymatic activities were assayed with 10 μM ATP in 384-well plates using the luminescent ADP-Glo™ assay (Promega, Madison, WI, USA), as previously described by our team [16,17], according to the recommendations of the manufacturer (see [23] for details on this method).

4. Conclusions

Taking into account our previous studies, using the biological active quinoxaline-2-carboxylic acid scaffold, we designed and synthesized a new potassium 6-oxo-7,13,16,22-tetraazatetracyclo[12.6.2.1^{8,12}.0^{17,21}]tricosa-1(20),8(23),9,11,14,16,18,21-octaen-2-yne-15-carboxylate **8** and then evaluated its anti-Pim-1/2 kinase activity. This macrocyclic quinoxaline **8** exhibited submicromolar activity on Pim-1 and Pim-2, with a significantly improved selectivity profile on the panel of human protein kinases studied in comparison to lead compound **1** and the reference drug SGI-1776. This compound could therefore represent a new attractive candidate for extending further pharmacomodulation studies and pharmacological investigations.

Supplementary Materials: The following supporting information can be downloaded at the website of this paper posted on Preprints.org, ^{1}H NMR, ^{13}C NMR, and HRMS.

Author Contributions: Conceptualization, C.D.-S. and C.L.; methodology, C.D.-S., C.B. M.-C.V.-M., and N.J.; investigation, C.B., S.L., C.L., C.D.-S., J.G., N.P., T.R. and S.B.; writing—original draft preparation, C.D.-S. and C.B.; writing—review and editing, C.D.-S.; supervision, C.D.-S.; project administration, C.D.-S.; funding acquisition, C.D.-S. All authors have read and agreed to the published version of the manuscript.

Funding: This work was funded by a grant from the Centre-Val de Loire Region and from the French National Research Agency under the program "Investissements d'avenir" Grant Agreement LabEx SynOrg (ANR-11-LABX-0029). The authors also thank the Cancéropôle Grand Ouest (3MC network—Marine Molecules, Metabolism and Cancer), GIS IBiSA (Infrastructures en Biologie Santé et Agronomie) and Biogenouest (Western France life science and environment core facility network) for supporting the KISSf screening facility. C. Blouet thanks the Centre-Val de Loire Region and the LabEx SynOrg for her PhD fellowship.

Acknowledgments: The authors would like to thank Cyril Colas from the "Fédération de Recherche" ICOA/CBM (FR2708)" for HRMS analysis, and Cécile Croix, from CEPR, for NMR spectrometry and technical support.

Conflicts of Interest: The authors declare no conflict of interest.

References

1. Mochizuki, T.; Kitanaka, C.; Noguchi, K.; Muramatsu, T.; Asai, A.; Kuchino, Y. Physical and Functional Interactions between Pim-1 Kinase and Cdc25A Phosphatase. Implications for the Pim-1-Mediated Activation of the c-Myc Signaling Pathway. *J. Biol. Chem.* **1999**, *274*, 18659–18666. https://doi.org/10.1074/jbc.274.26.18659.
2. Bachmann, M.; Kosan, C.; Xing, P.X.; Montenarh, M.; Hoffmann, I.; Möröy, T. The Oncogenic Serine/Threonine Kinase Pim-1 Directly Phosphorylates and Activates the G2/M Specific Phosphatase Cdc25C. *Int. J. Biochem. Cell Biol.* **2006**, *38*, 430–443. https://doi.org/10.1016/j.biocel.2005.10.010.
3. Theo Cuypers, H.; Selten, G.; Quint, W.; Zijlstra, M.; Maandag, E.R.; Boelens, W.; van Wezenbeek, P.; Melief, C.; Berns, A. Murine Leukemia Virus-Induced T-Cell Lymphomagenesis: Integration of Proviruses in a Distinct Chromosomal Region. *Cell* **1984**, *37*, 141–150. https://doi.org/10.1016/0092-8674(84)90309-X.
4. Maja Narlik-Grassow, Carmen Blanco-Aparicio, and A.C. The PIM Family of Serine/Threonine Kinases in Cancer. *Med. Res. Rev.* **2014**, *34*, 136–159. https://doi.org/10.1002/med.
5. Toth, R.K.; Warfel, N.A. Targeting PIM Kinases to Overcome Therapeutic Resistance in Cancer. *Mol. Cancer Ther.* **2021**, *20*, 3–10. https://doi.org/10.1158/1535-7163.MCT-20-0535.
6. Keane, N.A.; Reidy, M.; Natoni, A.; Raab, M.S.; O'Dwyer, M. Targeting the Pim Kinases in Multiple Myeloma. *Blood Cancer J.* **2015**, *5(7)*, e325. https://doi.org/10.1038/bcj.2015.46.

7. Amson, R.; Sigaux, F.; Przedborski, S.; Flandrin, G.; Givol, D.; Telerman, A. The Human Protooncogene Product P33pim Is Expressed during Fetal Hematopoiesis and in Diverse Leukemias. *Proc. Natl. Acad. Sci. U. S. A.* **1989**, *86*, 8857–8861. https://doi.org/10.1073/pnas.86.22.8857.
8. Koblish, H.; Li, Y. long; Shin, N.; Hall, L.; Wang, Q.; Wang, K.; Covington, M.; Marando, C.; Bowman, K.; Boer, J.; et al. Preclinical Characterization of INCB053914, a Novel Pan-PIM Kinase Inhibitor, Alone and in Combination with Anticancer Agents, in Models of Hematologic Malignancies. *PLoS One* **2018**, *13*, 1–22. https://doi.org/10.1371/journal.pone.0199108.
9. Czardybon, W.; Windak, R.; Gołas, A.; Gałezowski, M.; Sabiniarz, A.; Dolata, I.; Salwińska, M.; Guzik, P.; Zawadzka, M.; Gabor-Worwa, E.; et al. A Novel, Dual Pan-PIM/FLT3 Inhibitor SEL24 Exhibits Broad Therapeutic Potential in Acute Myeloid Leukemia. *Oncotarget* **2018**, *9*, 16917–16931. https://doi.org/10.18632/oncotarget.24747.
10. Bellon, M.; Nicot, C. Targeting Pim Kinases in Hematological Cancers: Molecular and Clinical Review. *Mol. Cancer* **2023**, *22*, 1–25. https://doi.org/10.1186/s12943-023-01721-1.
11. Qu, Y.; Zhang, C.; Du, E.; Wang, A.; Yang, Y.; Guo, J.; Wang, A.; Zhang, Z.; Xu, Y. Pim-3 Is a Critical Risk Factor in Development and Prognosis of Prostate Cancer. *Med. Sci. Monit.* **2016**, *22*, 4254–4260. https://doi.org/10.12659/MSM.898223.
12. Mikkers, H.; Nawijn, M.; Allen, J.; Brouwers, C.; Verhoeven, E.; Jonkers, J.; Berns, A. Mice Deficient for All PIM Kinases Display Reduced Body Size and Impaired Responses to Hematopoietic Growth Factors. *Mol. Cell. Biol.* **2004**, *24*, 6104–6115. https://doi.org/10.1128/mcb.24.13.6104-6115.2004.
13. An, N.; Kraft, A.S.; Kang, Y. Abnormal Hematopoietic Phenotypes in Pim Kinase Triple Knockout Mice. *J. Hematol. Oncol.* **2013**, *6*, 1. https://doi.org/10.1186/1756-8722-6-12.
14. Kumar, A.; Mandiyan, V.; Suzuki, Y.; Zhang, C.; Rice, J.; Tsai, J.; Artis, D.R.; Ibrahim, P.; Bremer, R. Crystal Structures of Proto-Oncogene Kinase Pim1: A Target of Aberrant Somatic Hypermutations in Diffuse Large Cell Lymphoma. *J. Mol. Biol.* **2005**, *348*, 183–193. https://doi.org/10.1016/j.jmb.2005.02.039.
15. Bullock, A.N.; Russo, S.; Amos, A.; Pagano, N.; Bregman, H.; Debreczeni, J.É.; Lee, W.H.; von Delft, F.; Meggers, E.; Knapp, S. Crystal Structure of the PIM2 Kinase in Complex with an Organoruthenium Inhibitor. *PLoS One* **2009**, *4(10)*, e7112, . https://doi.org/10.1371/journal.pone.0007112.
16. Oyallon, B.; Brachet-Botineau, M.; Logé, C.; Robert, T.; Bach, S.; Ibrahim, S.; Raoul, W.; Croix, C.; Berthelot, P.; Guillon, J.; et al. New Quinoxaline Derivatives as Dual Pim-1/2 Kinase Inhibitors: Design, Synthesis and Biological Evaluation. *Molecules* **2021**, *26*, 867. https://doi.org/10.3390/molecules26040867.
17. Oyallon, B.; Brachet-Botineau, M.; Logé, C.; Bonnet, P.; Souab, M.; Robert, T.; Ruchaud, S.; Bach, S.; Berthelot, P.; Gouilleux, F.; et al. Structure-Based Design of Novel Quinoxaline-2-Carboxylic Acids and Analogues as Pim-1 Inhibitors. *Eur. J. Med. Chem.* **2018**, *154*, 101–109. https://doi.org/10.1016/j.ejmech.2018.04.056.
18. Liang, Y.; Fang, R.; Rao, Q. An Insight into the Medicinal Chemistry Perspective of Macrocyclic Derivatives with Antitumor Activity: A Systematic Review. *Molecules* **2022**, *27(9)*, 2837. https://doi.org/10.3390/molecules27092837.
19. Basit, S.; Ashraf, Z.; Lee, K.; Latif, M. First Macrocyclic 3rd-Generation ALK Inhibitor for Treatment of ALK/ROS1 Cancer: Clinical and Designing Strategy Update of Lorlatinib. *Eur. J. Med. Chem.* **2017**, *134*, 348–356. https://doi.org/10.1016/j.ejmech.2017.04.032.
20. Verstovsek, S.; Komrokji, R.S. A Comprehensive Review of Pacritinib in Myelofibrosis. *Futur. Oncol.* **2015**, *11*, 2819–2830. https://doi.org/10.2217/fon.15.200.
21. Mahesh, R.; Dhar, A.K.; Sasank T.v.n.v., T.; Thirunavukkarasu, S.; Devadoss, T. Citric Acid: An Efficient and Green Catalyst for Rapid One Pot Synthesis of Quinoxaline Derivatives at Room Temperature. *Chinese Chem. Lett.* **2011**, *22*, 389–392. https://doi.org/10.1016/j.cclet.2010.11.002.
22. Mahesh, R.; Devadoss, T.; Dhar, A.K.; Venkatesh, S.M.; Mundra, S.; Pandey, D.K.; Bhatt, S.; Jindal, A.K. Ligand-Based Design, Synthesis, and Pharmacological Evaluation of 3-Methoxyquinoxalin-2-Carboxamides as Structurally Novel Serotonin Type-3 Receptor Antagonists. *Arch. Pharm. (Weinheim).* **2012**, *345*, 687–694. https://doi.org/10.1002/ardp.201200038.
23. Zegzouti, H.; Zdanovskaia, M.; Hsiao, K.; Goueli, S.A. ADP-Glo: A Bioluminescent and Homogeneous Adp Monitoring Assay for Kinases. *Assay Drug Dev. Technol.* **2009**, *7*, 560–572. https://doi.org/10.1089/adt.2009.0222.
24. Blanco-Aparicio, C.; Carnero, A. Pim Kinases in Cancer: Diagnostic, Prognostic and Treatment Opportunities. *Biochem. Pharmacol.* **2013**, *85*, 629–643. https://doi.org/10.1016/j.bcp.2012.09.018.
25. Supplementary X-ray crystallographic data: Cambridge Crystallographic Data Centre, University Chemical Lab, Lensfield Road, Cambridge, CB2 1EW, UK. Available online: https://www.ccdc.cam.ac.uk/ (accessed 15 May 2023).

26. Sheldrick, G.M. (1996) SADABS, University of Göttingen, Germany.
27. Sheldrick, G.M. A short history of SHELX. Acta Crystallogr. Sect. A **2008**, *64*, 112–122. https://doi.org/10.1107/S0108767307043930.